

RESEARCH ON PROPERTIES OF Fe-BASED POWDER METALLURGY MATERIAL STRENGTHENED BY BORIDING

H. M. Fang^{a,b,1} and F. Xu^a

UDC 539.4

The pack boriding process of Fe-based powder compact was carried out at 850 to 1050°C for 3 to 10 h. The microstructure and the thickness of the boride layer were observed by VHX-6000 ultra-depth microscopic three-dimensional microscope. The surface hardness of the boride layer was measured by a Rockwell hardness tester, the phase composition of the boride layer was analyzed by X-ray diffractometer and the friction and wear properties of the sample were tested on the MMW-2 friction and wear tester. The worn surfaces of boride layer was observed by scanning electron microscope. The results show that the boride layer was mainly composed of Fe₂B single phase, and its thickness was uniform and firmly bonded to the substrate. The thickness and hardness of the layer gradually increased with time and temperature. The binding force between the layer and the substrate would be decreased while the thickness of the layer was too thin or too thick. Boriding at 850, 900, and 950°C resulted with formation of Fe₂B phase while FeB and Fe₂B phases occurred at 1050°C. The thickness of the layer in a suitable range could improve the wear properties of the material.

Keywords: pack boride, Fe-based powder metallurgy material, abrasion loss, friction and wear, surface hardness.

Introduction. Fe-based powder metallurgy materials have great application potential. They are rapidly developed and widely used in machinery, aerospace, agricultural machinery, especially in the automotive industry. With the development of modern industry and technology. The problem like improve the hardness the wear resistance of the surface of powder metallurgy materials was urgently needed to be solved in the use of powder metallurgy materials [1]. Surface modification of powder metallurgy materials has gradually become an important field of material science research. At present, the surface modification technologies include surface mechanical strengthening technology, laser surface strengthening technology and surface chemical heat treatment technology, etc. The mainly researches of the latter were to improve the surface hardness and wear resistance of the material by nitriding, carburizing, and carbonitriding and to improve the corrosion resistance and high temperature oxidation resistance by infiltrating silicon, chromizing, aluminizing on the surface of the material [2]. Through analysis and comparison, the solid powder boride is an ideal method that can meet the process and economy, which is included in the chemical heat treatment method on the surface of powder metallurgy materials [3–6].

In this paper, the surface of Fe-based powder metallurgy materials is chemically strengthened by solid powder method. The thickness and surface hardness, phase composition and friction and wear properties of the layer were studied to expand the use of Fe-based powder metallurgy materials.

1. Experiment.

1.1. Materials and Methods of Experiment. The Fe-based powder metallurgy material was used as the substrate and its main component (by mass fraction) is: 3% C + 0.2% Si + 0.2% Ni + 0.1% Al + 0.1% Mn + 96.4% Fe,

^aCollege of Mechanical and Electrical Engineering, Nanjing University of Aeronautics and Astronautics, Nanjing, China (10122000353@ahcme.edu.cn). ^bCollege of Mechanical Engineering, Anhui Technical College of Mechanical and Electrical Engineering, Wuhu, China. Translated from Problemy Prochnosti, No. 4, pp. 138 – 144, July – August, 2020. Original article submitted October 28, 2019.

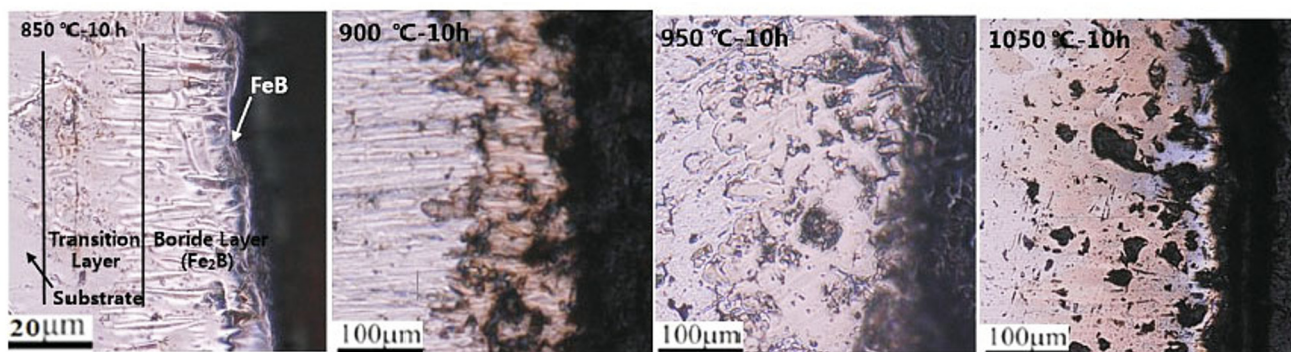


Fig. 1. The morphology of boride layer of specimens with different temperature for 10 h.

which was the raw material for sintering boride research, all the powder is mixed by element mixing method on a planetary ball mill and the mixed powder was pressed on a hydraulic press to obtain a compaction. Finally, sintering and boride are carried out in a high temperature furnace, the detailed process will be described later.

1.2. Experimental Method. The materials above were mixed on a ball mill with speed of 300 rpm for over 6 h. The mixture is pressed to a size of $\varnothing 20 \times 10$ mm at a pressure of 650 MPa. The specimen is embedded in solid powder, placed in corundum crucible and sealed and dried. The crucible is placed in a high temperature furnace at the temperature of 850–1050°C for 3 to 10 h, then cooled to the normal room temperature in the air. The corundum crucible is sealed by the high-temperature glue with model number 8317, that could resistant high-performance 1800°C, which can prevent the material from oxidizing at high temperature effectively.

1.3. The Layer Structure and Performance. The metallographic structure of the boride layer was observed by VHX-6000 ultra-depth microscopic three-dimensional microscope. The surface hardness of the specimen was measured by HR-150A Rockwell hardness tester. D8-FOCUS X-ray diffractometer was used (anode is Cu target, $\lambda = 0.125$ nm) X-ray diffraction (XRD) analysis of the surface of the boride layer and the surface of the layer after friction and wear. The Fe-based material and the friction pair material (45 quenched steel) were tested on the MMW-2 friction and wear test machine according to the load of 368 g and the rotation speed of 100 rpm, and the average friction coefficient and the wear rate were calculated. The friction torque is automatically collected by the system, and the friction factor is obtained by conversion. The amount of abrasion loss is measured by an electron microscopic balance. The worn surfaces of the boride layer after wear test was observed by SU8000 scanning electron microscope (SEM). All experimental data are average values of the measured values under three identical conditions.

2. Results and Analysis.

2.1. Metallographic Structure Observation and Analysis. The metallographic structure of the boride layer of the Fe-based material maintained at 850, 900, 950, and 1050°C for 10 h is shown in Fig. 1. The layer is continuous and firmly bonded to the substrate. It can be seen from Fig. 1 that the specimen structure from the inside to the outside is composed of the substrate, the transition layer and the boride layer. The inner layer is dense while the surface is loose, and there are minute voids and microcracks, which is particularly obvious at 1050°C.

The tooth shape of the boride layer was very thin when the specimen at the sintering temperature of 850°C for 10 h, and it was inserted into the substrate with a needle-like shape, the thickness of the layer was thin at this time. As the sintering temperature is increased from 850 to 1050°C, the tooth shape of the boride is gradually thickened and joined together, and the thickness is gradually increased. However, as temperature increases, it is easier to form pores and looseness that are detrimental to the properties in the boride layer [7–10].

2.2. Thickness and Analysis of Boride Layer. The effect of sintering time on the thickness of boride layer at 900°C is showed in Fig. 2, and the effect of sintering temperature on the thickness of boride layer is showed in Fig. 3. The thickness of the boride layer increases as the sintering temperature and sintering time increased. Since B atoms have a very low solid solubility in Fe, a very small amount of B can form a compound with iron. Boriding is a process of reaction-diffusion. When the temperature increases, the diffusion speed of B atoms increases, and the

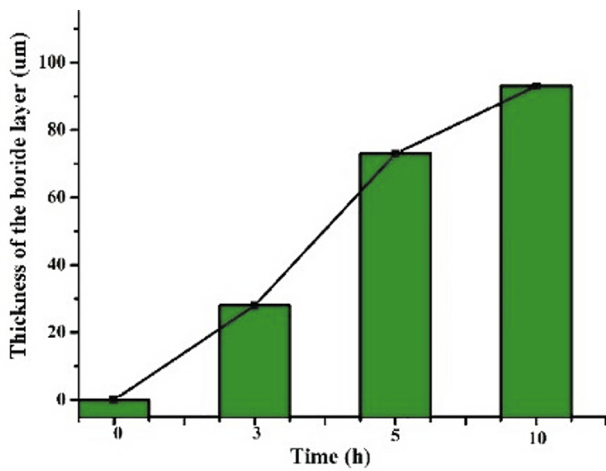


Fig. 2

Fig. 2. The thickness of boride layer at 900°C for different time.

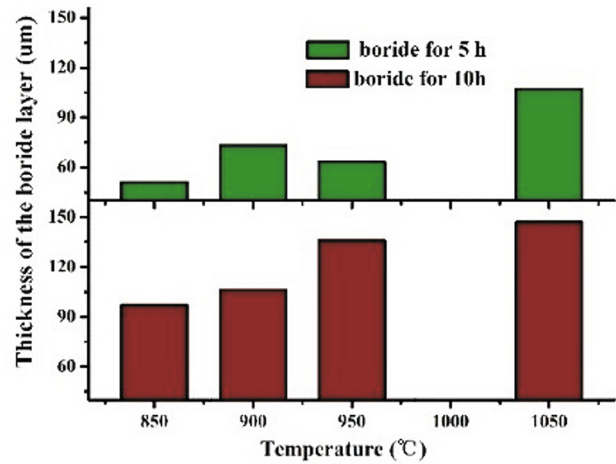


Fig. 3

Fig. 3. The thickness of boride layer of specimens with different processes.

thickness of the layer becomes thicker. The longer the time, the thickness of the layer also increases accordingly. Therefore, the increase of both will lead to an increase in the thickness of the layer [11].

It can be seen from Fig. 3 that the thickness of the layer of the specimen is 78 µm at 900°C for 5 h, compared with 28 µm for the 3 h specimen, the thickness of the layer is increased by 1.78 times. The thickness of the layer for 10 h compared with the holding time of 5 h was only increased by 0.24 times. From this, it can be seen that during the first 5 h, the thickness of the layer increased significantly, and then the time was extended, and the thickness increase began to become slow. Under the experimental conditions, the holding time can be about 5 h, and the excessive extension time will increase the energy consumption, which is not recommended in terms of economy and environmental protection.

It can be seen from Fig. 3 that the thickness of the specimen layer at a sintering temperature of 1050°C and a holding time of 10 h is 147 µm, which is almost 900°C of the sintering temperature and 1.5 times that of the specimen with the same holding time. However, from the metallographic structure of the boride layer in Fig. 1, the pores and looseness appear in the former layer and the friction coefficient of the specimen is unstable combined with the subsequent friction and wear test, its wear loss is large during the test. The wear performance is not as good as the latter. The specimen with holding time of 5 h has a thickness of 107 µm at 1050°C and a thickness of 73 µm at 900°C. However, it can be seen in Fig. 4 that the surface hardness of the two is not much different. Therefore, the sintering temperature of this experiment should not be too high. Referring to the metallographic structure showed in Fig. 1, the density of the layer is lowered because of the pores and looseness existing in the layer is increased. The sintering temperature can be about 900°C under the experimental conditions, and a boride layer about 100 µm can be obtained. The substrate material is also sufficiently sintered while obtaining the boride layer [12].

2.3. Hardness and XRD Analysis of Boride Layer. After the high temperature boride of the Fe-based specimen, the effect of sintering time and sintering temperature on the surface hardness of the boride layer is shown in Fig. 5. The surface hardness gradually increases with the increase of sintering temperature. The surface hardness of the specimen with the sintering time of 10 h was always higher than that of the specimen with the sintering time of 5 h. It can be seen that the surface hardness also increased with the increase of the sintering time. This has a positive correspondence with the thickness curve of the layer of Fig. 5.

The specimen with at 1050°C for 10 h has a surface Rockwell hardness of 80, which is 50% higher than the specimen at 900°C for same time. However, the increase of the thickness of the layer and the increase of the surface hardness will lead to an increase in the brittleness of the boride layer, which is not good for the mechanical properties and friction and wear of the specimen. When subjected to a large impact force, the layer is easily peeled off and cracked. This is because the coefficient of thermal expansion differs greatly between the boride layer and the

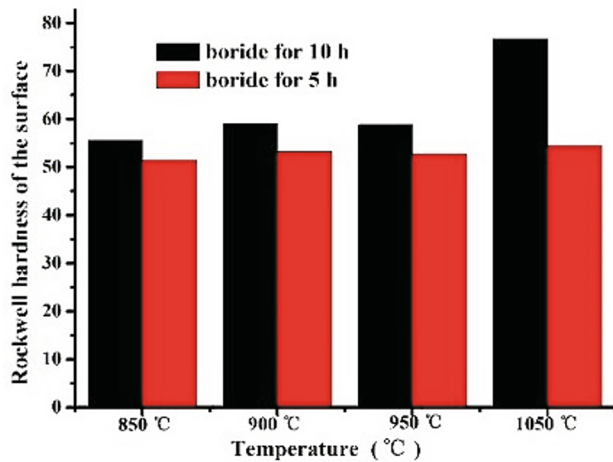


Fig. 4

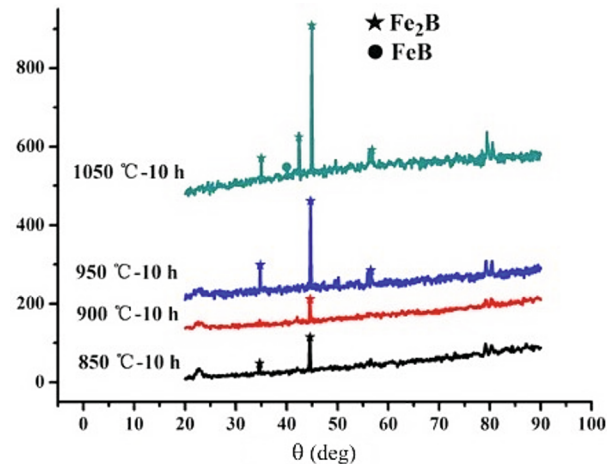


Fig. 5

Fig. 4. The surface hardness of specimens with different processes.

Fig. 5. XRD patterns of boride layer of specimens at different temperature for 10 h.

substrate, and the Fe-boron compound in the boride layer is a hard and brittle intermetallic compound, which is prone to adverse internal stress under stress and temperature changes.

The X-ray patterns of the boride layer of specimen after at different temperatures is shown in Fig. 5. It can be seen that the diffraction peaks at 850–950°C are basically Fe_2B phases with almost no FeB phase. This is because the FeB phase is formed on the surface in a high B atmosphere. When the temperature is raised, the B atom has a strong diffusion ability and easily diffuses into substrate, resulting in almost no FeB formed in the layer. The solubility of B in Fe is extremely low at high temperature, and the Fe_2B phase is formed quickly on the surface. If the sintering temperature is increased or the time of boride treatment is prolonged, more FeB with a higher B content will be formed [13–15]. The powder particulate material of this experiment usually has defects such as pores, which form a path in the compact, which increases the permeability of the B atoms and reducing the activation energy of diffusion. It is beneficial to the growth of Fe_2B phase but this diffusion ability is limited. When the temperature rises to 1050°C, the FeB phase will be appeared. The result is consistent with the metallographic structure of the boride layer in Fig. 1.

2.4. Friction and Wear Test and Results. The experimental is mainly studied the wear properties of boride specimens under dry sliding, and the directly sintered specimens is compared (unboride specimen), which is prepared by sintering at 1000°C for 3 h with a pressure of 3.5–5.5 MPa. Figure 6 shows the friction coefficient curve of boride specimens at 850, 900, and 1050°C for 10 h. It can be seen that all the friction coefficient of boride specimens is higher than that of unborided specimen. That is because unborided specimen has lower oxidation resistance. The oxide layer produced on the surface when the temperature of the frictional contact area increases which is equivalent to the “solid lubricant” with the function of lubrication and wear reduction. So the friction coefficient of it is relatively low. The abrasion loss of the unborided specimen is significantly higher than that of the other boride specimen in Fig. 7, which indicate that a suitable boride process can reduce the abrasion and improve the wear resistance of the material. Figure 8 shows that the surface of the unborided specimen is sharply worn after test. Lacerated morphology can be observed on the surface between the oxide layer and the substrate, many microcracks are appeared on the worn surface, which is indicated in Fig. 8.

The lowest friction coefficient of boride specimen is seen at 900°C for 10 h. The friction coefficient curve rises slowly to about 0.6 in the first 18 min, and then remains relatively stable. This indicates that the surface layer has not lost its characteristics and has not suffered significant damage. The undamaged wear track on the SEM image shown in Fig. 8 supports this situation with the friction coefficient. The coefficient of friction of the boride specimens at 850°C for 10 h and 1050°C for 10 h is higher than that of the 900°C and the curves fluctuate sharply. Their high friction coefficient values can be explained by the SEM wear images shown in Fig. 8. Microcracks formed

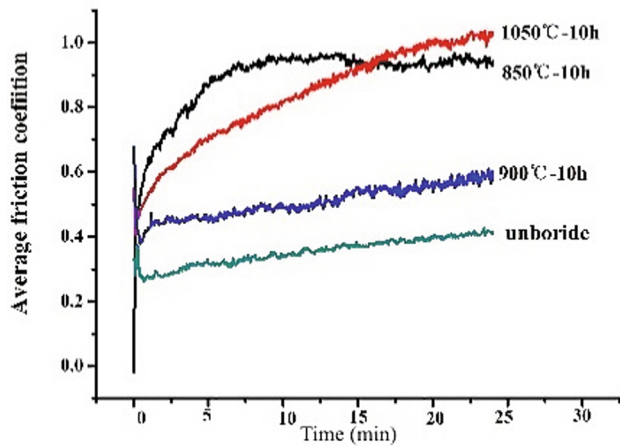


Fig. 6

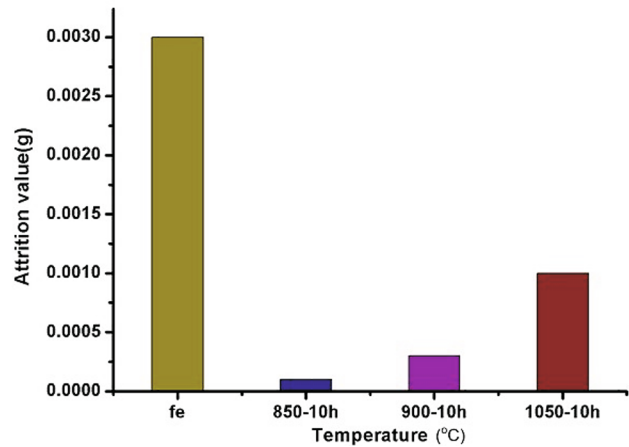


Fig. 7

Fig. 6. The friction coefficient of specimens at different temperature for 10 h.

Fig. 7. The attrition value at different temperature for 10 h in wear tests.

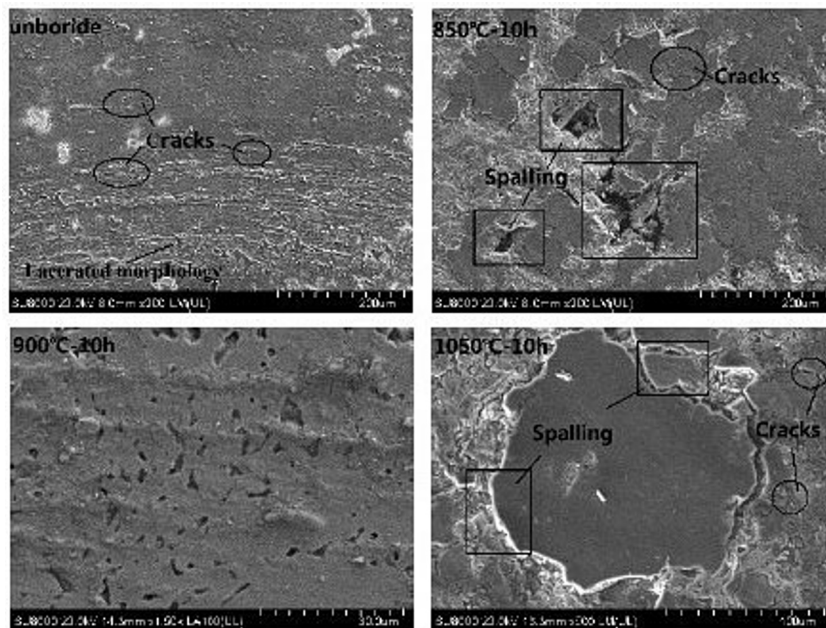


Fig. 8. SEM micrographs of the worn surfaces for wear tests.

by fatigue caused by stress under cyclic loading and damage caused by cracking and plastic deformation caused by the development of these cracks result in high friction coefficient and high fluctuation.

In the experiment, the specimen at 850°C resulting in a thin layer because it's low sintering temperature. The applied load causes the fracture and the spalling of the boride layer. The peeled layer not only cause a large abrasion loss but also be crushed into hard particles on the wear surface, and the friction coefficient is instantaneously increased, which is consistent with the friction coefficient of the specimen at 850°C in Fig. 6 with high fluctuation. The loose layer with more pores is obtained at 1050°C, the structure of the layer becomes smooth, the adhesion between the layer and the substrate is weakened, and is easily cracked and peeled off in the wear test. All these poor properties resulting in a high abrasion loss in Fig. 7.

So, the thickness of the boride layer has an optimal range, if the layer is too thick or too thin, it is easy to peel off. It is necessary to select an appropriate holding time according to different sintering temperatures to achieve a sufficient thickness of the infiltrated layer for the selection of boride process parameters.

CONCLUSIONS

1. The metallographic structure of the boride layer is followed by boride layer (Fe_2B), transition layer and substrate. the boride layer formed on the surface is uniform and compact, which is inserted into the substrate needle tooth shape and combined with it. As the sintering temperature and the sintering time increases, the shape of the boride layer gradually becomes smoother.

2. The sintering temperature and sintering time are closely related to the thickness of the layer, and the increase of both will lead to an increase in the thickness of the layer. And there are pores and looseness in the layer, which is more obvious when the sintering temperature is higher.

3. The thickness of the boride layer has an optimal range. Ensuring the thickness of the layer within a suitable rang by controlling the sintering temperature, sintering time and other process parameters, which is beneficial to the properties of the material.

Acknowledgments. This work is funded by the Natural Science Foundation of China (51575269), the University Natural Science Foundation of Anhui (KJ2017ZD50), the University support program for young talents of Anhui (gxyq2019186).

REFERENCES

1. I. Campos-Silva, M. Ortiz-Domínguez, N. López-Perrusquia, et al., "Characterization of AISI 4140 borided steels," *Appl. Surf. Sci.*, **256**, No. 8, 2372–2379 (2010).
2. Y. S. Zhu, W. Z. Lu, D. W. Zuo, et al., "Characteristics of RE-B surface diffusion process on the new damage tolerance TC21 alloy," *Rare Metal Mater. Eng.* [in Chinese], **43**, No. 3, 693–697 (2014).
3. A. G. von Matuschka, *Boronizing*, Carl Hanser Verlag, Munich (1980).
4. I. Uslu, H. Comert, M. Ipek, et al., "Evaluation of borides formed on AISI P20 steel," *Mater. Design*, **28**, No. 1, 55–61 (2007).
5. S. C. Singhal, "A hard diffusion boride coating for ferrous materials," *Thin Solid Films*, **45**, No. 2, 321–329 (1977).
6. V. D. Yakhnina, A. M. Kozlov, and A. I. Luk'yanitsa, "Physicochemical characteristics of powder boronizing," *Powder Metall. Met. Ceram.*, **18**, No. 4, 237–240 (1979).
7. S. Sen, U. Sen, and C. Bindal, "Tribological properties of oxidised boride coatings grown on AISI 4140 steel," *Mater. Lett.*, **60**, Nos. 29–30, 3481–3486 (2006).
8. H. G. Kariofillis, G. E. Kiourtsidis, and D. N. Tsipas, "Corrosion behavior of borided AISI H13 hot work steel," *Surf. Coat. Tech.*, **201**, Nos. 1–2, 19–24 (2006).
9. V. I. Dybkov, W. Lengauer, and K. Barmak, "Formation of boride layers at the Fe–10% Cr alloy–boron interface," *J. Alloy. Compd.*, **398**, Nos. 1–2, 113–122 (2013).
10. H. Cimenoglu, E. Atar, and A. Motallebzadeh, "High temperature tribological behavior of borided surfaces based on the phase structure of the boride layer," *Wear*, **309**, Nos. 1–2, 152–158 (2014).
11. A. H. Üçisik and C. Bindal, "Fracture toughness of boride formed on low-alloy steels," *Surf. Coat. Tech.*, **94–95**, 561–565 (1997).
12. M. Keddami and S. M. Chentouf, "A diffusion model for describing the bilayer growth ($\text{FeB}/\text{Fe}_2\text{B}$) during the iron powder-pack boriding," *Appl. Surf. Sci.*, **252**, No. 2, 393399 (2005).
13. G. Palombarini and M. Carbucicchio, "Growth of boride coatings on iron," *J. Mater. Sci. Lett.*, **6**, No. 10, 415–416 (1987).
14. E. Medvedovski, "Formation of corrosion-resistant thermal diffusion boride coatings," *Adv. Eng. Mater.*, **18**, No. 1, 11–33 (2016).
15. O. A. Gómez-Vargas, M. Keddami, and M. Ortiz-Domínguez, "Kinetics and tribological characterization of pack-borided AISI 1025 steel," *High Temp. Mater. Proc.*, **36**, No. 3, 197–208 (2017).